The application of EOF in the analysis of the variability of water temperature, salinity and density in selected regions of the Norwegian Sea

ANDRZEJ JANKOWSKI
Institute of Oceanology,
Polish Academy of Sciences,
Sopot

Abstract

The results of applying empirical orthogonal functions (EOF) to the decomposition and approximation of vertical profiles of seawater temperature, salinity and density are presented. The calculated empirical orthogonal functions were used to analyse the spatial and temporal variability of hydrophysical parameters along two hydrographical transects in selected regions of the Norwegian Sea.

1. Introduction

Empirical orthogonal functions (EOF) have been widely applied in investigations into the field structure of physical parameters of the Earth's atmosphere. The first papers on EOF were published in the late 1950s and early 1960s (Holmstrom, 1963; Lorenz, 1956; Obukhov, 1960). In oceanological research, EOF have been used in studies of sea level (Nielsen, 1979; Wróblewski, 1984; 1986; 1990), and currents (Korotayev et al., 1978; Kundu et al., 1975; Vasilenko and Mirabel, 1976). A monograph on EOF has been written (Preisendorfer, 1988), discussing its theoretical aspects and describing its many practical applications in studies of the atmosphere and ocean.

In the present study an attempt was made to use EOF to analyse the variability and describe the vertical structure of seawater temperature, salinity and density fields in selected regions of the Norwegian Sea. With the aid of EOF the spatial distribution of hydrological parameters can be visualised in ' condensed ' form and the components of different variance characterising

the variability of a physical quantity can be analysed. It is these properties of EOF that suggest they could be used as an additional, nonstandard tool in the processing of *in situ* measurement data.

This paper is arranged as follows. Section 2 presents basic information on EOF and the methodology of their implementation, as well as technical details of the measurements used here. Section 3 discusses the application of EOF in analysis of the vertical structure of seawater temperature, salinity and density fields. Section 4 compares the structure of the water temperature, salinity and density fields in selected regions of Norwegian Sea in the summers of 1988, 1989 and 1991 (the measurement data were obtained during cruises of r/v 'Oceania'). The final section summarises and comments on the use of EOF in the analysis of hydrophysical parameters.

2. Methodology and empirical material

2.1. The EOF method

Consider the *in situ* data of any hydrophysical quantity $\Phi_i^*(z_j)$ measured at a series of measurement stations: $i = 1, ..., N$, and recorded at M levels in the water z_j; $j = 1, ..., M$. For this set of measurement stations a mean vertical profile is determined:

$$\bar{\Phi}(z_j) = \frac{1}{N} \sum_{k=1}^{N} \Phi_k^*(z_j), \qquad\qquad j = 1, ..., M \qquad (1)$$

as are vertical profiles of fluctuations with respect to the calculated mean profile:

$$\Phi_i(z_j) = \Phi_i^*(z_j) - \bar{\Phi}(z_j), \qquad i = 1, ..., N; \ \ j = 1, ..., M. \qquad (2)$$

Fluctuation profiles $\Phi_i(z_j)$ are approximated by expanding them into a series of functions:

$$\Phi_i(z_j) = \sum_{k=1}^{M} h_k(z_j)\beta_{ik}, \qquad i = 1, ..., N; \ \ j = 1, ..., M. \qquad (3)$$

Functions $h_i(z_j)$ should fulfil the conditions of orthogonality and be normalised, *i.e.*

$$\sum_{j=1}^{M} h_i(z_j)h_k(z_j) = M\delta_{ik}, \qquad i, k = 1, ..., M \qquad (4)$$

where:

$$\delta_{ik} = \begin{cases} 0 & for \ \ i \neq k \\ 1 & for \ \ i = k. \end{cases}$$

Functions h_j and coefficients β_{ik} should be chosen in such a way that expansion (3) best approximates the vertical fluctuation profile $\Phi_i(z_j)$ (2).

In expansion (3) functions $h_k(z_j)$ express the fluctuation variability $\Phi_i(z_j)$ relative to the vertical coordinate z ($z_j, j = 1, ...M$). Coefficients β_{ik} describe the fluctuation variability $\Phi_i(z_j)$ with respect to the horizontal coordinate x ($x_i; i = 1, ...N$, – position of station), thereby characterising the scale and amplitude of the variability of a vertical profile. The fluctuation variability of a physical quantity is thus separated into a quotient of two functions describing the fluctuation variability in the vertical only or in the horizontal only. Discrete functions h_k satisfying condition (4) are called modes or main components, while their corresponding coefficients β_{ik} are known as amplitude functions, or simply, amplitudes (Preisendorfer, 1988).

In the EOF method, functions h_k are chosen as eigenfunctions (eigenvectors) of the covariance matrix of fluctuations $\Phi_i(z_j)$

$$c(z_i, z_j) = \frac{1}{N} \sum_{k=1}^{N} \Phi_k(z_i)\Phi_k(z_j), \qquad i, j = 1, ..., M \qquad (5)$$

which are also solutions of the equation

$$\sum_{i=1}^{M} c(z_i, z_j)h_k(z_i) = \lambda_k h_k(z_j), \qquad j, k = 1, ..., M \qquad (6)$$

where

λ_k = eigenvalues of the covariance matrix $c(z_i, z_j)$.

By selecting the eigenfunctions of the matrix $c(z_i, z_j)$ i.e. $h_k(z_j)$ for the consecutive eigenvalues λ_k, in decreasing order of magnitude, the fluctuation field $\Phi_i(z_j)$ (2) can be approximated to the following form:

$$\hat{\Phi}_i(z_j) = \sum_{k=1}^{L} h_k(z_j)\beta_{ik}, \qquad i = 1, ..., N; \; j = 1, ..., M \qquad (7)$$

where

$L \le M$ – the number of terms in expression (3).
Series (7) describes fluctuations $\Phi_i(z_j)$ with a minimum mean square error:

$$\delta = \frac{1}{N} \sum_{i=1}^{N} \frac{1}{M} \sum_{j=1}^{M} \left(\Phi_i(z_j) - \hat{\Phi}_i(z_j) \right)^2, \quad i = 1, ..., N; \; j = 1, ..., M. \quad (8)$$

Amplitudes β_{ik}, minimising the mean square error (8) of series (7), can be estimated from

$$\beta_{ik} = \sum_{j=1}^{N} \Phi_i(z_j)h_k(z_j), \qquad i = 1, ..., N; \; j = 1, ..., M. \qquad (9)$$

The amplitudes β_{ik} determined in this way also satisfy the orthogonality condition:

$$\frac{1}{N} \sum_{k=1}^{N} \beta_{ki}\beta_{kj} = \frac{1}{M}\lambda_i \delta_{ij}, \qquad\qquad i,j = 1, ..., M \qquad (10)$$

and their variance satisfies the following dependence:

$$\frac{1}{M}\lambda_j = \frac{1}{N} \sum_{k=1}^{N} \beta_{kj}^2, \qquad\qquad j = 1, ..., M. \qquad (11)$$

These properties of eigenfunctions $h_k(z_j)$ and amplitudes β_{ik} suggest their possible use as variability characteristics (modes) of the fluctuaction field $\Phi_i(z_j)$ expanded into a series. The individual eigenvectors and amplitudes corresponding to a given eigenvalue characterise the variability of a hydrological parameter with maximum variance, the measure of which is the given eigenvalue λ_j of the covariance matrix $c(z_i, z_j)$.

The convergence of expansion (7) determines the ratio of summed eigenvalues

$$\alpha(L) = \frac{1}{S_\lambda} \sum_{i=1}^{L} \lambda_i, \qquad\qquad L = 1, ..., M \qquad (12)$$

where

$$S_\lambda = \sum_{i=1}^{M} \lambda_i, \qquad\qquad\qquad (13)$$

characterises the relative value of the summed fluctuation variance with respect to the total fluctuation variance contained in the input data $\Phi_i^*(z_j)$. In practical calculations, values of $\alpha(L)$ are assumed to be of the order of $0.90 - 0.95$ ($90\% - 95\%$) (Nilsen, 1979; Wróblewski, 1984; 1986).

Eq. (11) shows the connection between amplitudes β_{ik} and eigenvalues λ_i of the covariance matrix. The eigenvalues are equal to the mean square of the amplitudes, and hence express the mean 'energy' (the pulsation square of the parameter in question) in particular modes. By means of eqs. (3), (4), (9) – (11) the following relation can be shown to occur:

$$\frac{1}{N} \sum_{k=1}^{N} \sum_{i=1}^{M} \Phi_k^2(z_i) = \frac{1}{N} \sum_{k=1}^{N} \sum_{j=1}^{M} \beta_{kj}^2(z_j) = \sum_{j=1}^{M} \lambda_j. \qquad (14)$$

It defines the relationship between eigenvalues λ_i, amplitudes β_{ik} and 'energy', expressed as the pulsation square of $\Phi_k^2(z_i)$. The contribution of each separate component of given variance to the variability of a hydrophysical parameter can thus be defined.

The physical sense of EOF can be explained as follows (Kundu et al., 1975; Preisendorfer, 1988). In situ measurements of a parameter at N measurement stations and M levels can be regarded as an element of a discrete M-dimensional space (M-dimensional vectors at N points of such a space).

The EOF are interpreted as the main directions (axes) of the data set in this M-dimensional space. The choice of main axes in such a space is analogous to considering the main axes of an inertia tensor in the mechanics of continuous media.

In this particular case the covariance matrix $c(z_i, z_j)$ (5) takes the part of the tensor. Diagonalisation of a real symmetrical matrix $c(z_i, z_j)$ produces orthogonal directions, on to which the set of N vectors is projected. Rearranging the eigenvalues in a series $\lambda_1 > \lambda_2 > ... > \lambda_M$ yields the axis with maximum variance corresponding to the eigenfunction of the matrix $c(z_i, z_j)$ – h_1 and the axis with minimum variance corresponding to the eigenfunction h_M. Mode h_1 contains the maximum energy of the entire data set. The next mode h_2 contains the maximum energy of what is left after the first mode has been hived off, *etc.* As a result a set of eigenfunctions and amplitudes are obtained characterising the uncorrelated components describing variability with decreasing variance, the sum of which expresses, with a minimum mean square error (8), the summed fluctuations contained in the input data set. A more detailed discussion of the physical significance of EOF wil be found in Kundu *et al.* (1975) and Preisendorfer (1988).

2.2. Empirical material

The results of vertical soundings of temperature and salinity performed during voyages of r/v ' Oceania' in the Norwegian and Greenland Seas in the summers of 1988, 1989 and 1991 have been used in this work. Two hydrographical transects were selected in two different (with respect to the hydrological conditions) regions of the Norwegian Sea:

- in the Faeroe-Shetland Channel,
- in the confluence zone between the Norwegian and Barents Seas (along longitude 15° E, from 70° N to 76° 30′ N).

The locations of measurement stations along these transects are shown in Fig. 1. Deep-water temperature and salinity measurements down to 1000 m were made during all three voyages with an identical CTD Guideline probe (model 8770) The absolute accuracy of the data after correction was <0.02°C for temperature and $< 0.01 \times 10^{-3}$ for salinity.

The transect regions are well-known for their complex hydrometeorology (Johannessen, 1986; Sukhovey, 1977). Analysis of the many environmental parameters measured during voyages of r/v ' Oceania' (Druet and Jankowski, 1992) indicates that the hydrological conditions in 1988 were quite different from those encountered the following year, very probably owing to the different hydrometeorological situation obtaining in the study
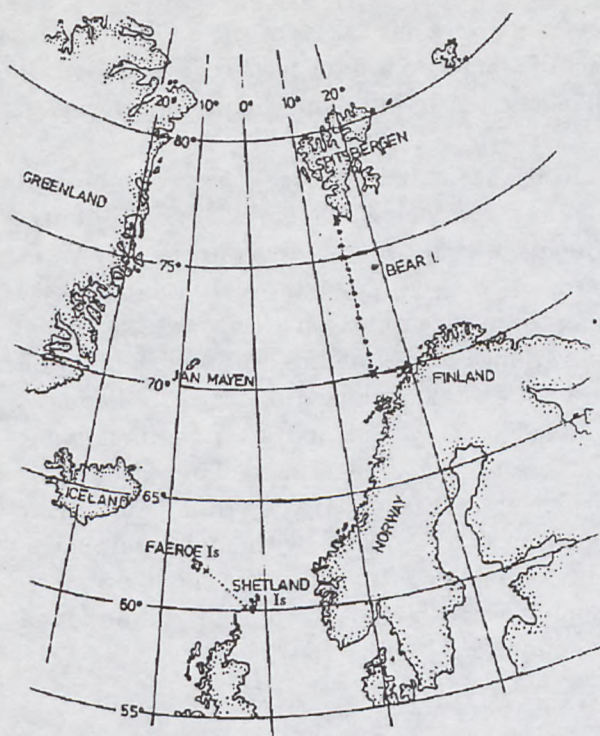
Fig. 1. Location of measurement stations in selected regions of the Norwegian Sea

area. The hydrometeorological conditions in the transect regions are discussed in greater depth in Johannessen (1986) and Sukhovey (1977); the conditions encountered by r/v 'Oceania' during her voyages are described in Druet and Jankowski (1991, 1992); Jankowski (1991a,b), Jankowski and Swerpel (1990), and in a collective paper (Druet, 1993).

2.3. Methodology of calculations

The results of vertical temperature and salinity soundings interpolated on a regular depth grid with a 5 m step were used in the calculations.

Values of the density σ_t[1] were determined from temperature and salinity measurements in accordance with UNESCO standards (UNESCO, 1983). Mean profiles (1) and fluctuations (2) for the various profiles at measurement stations were calculated for each parameter, transect and year. Following this, the covariance matrix of fluctuactions $c(z_i, z_j)$ (5), as well as

---

[1]density sigma − t (density 'excess') is expressed as $\sigma_t = \rho - 10^3 \text{kg m}^{-3}$, where: $\rho = \rho(T, S, p)$ − sea-water density; T − temperature; S − salinity, p − pressure.

its eigenvalues λ_i and eigenvectors h_i were calculated by Jacobi's method (Ralston, 1975). Amplitudes β_{ik} were then calculated using eq. (9), and by means of expansion (7) the fluctuations $\Phi_i(z_j)$ of the hydrophysical quantity were approximated. The full values of temperature, salinity and density were determined from

$$F_i(z_j) = \sum_{k=1}^{l} h_k(z_j)\beta_{ik} + \bar{\Phi}(z_j), \qquad l = 1, ..., L; \ i = 1, ..., N \qquad (15)$$

where

$\quad L$ = number of modes chosen in accordance with criterion (12),

$\quad F_i(z_j) = T_i(z_j), \ S_i(z_j)$ and $(\sigma_t)_i(z_j)$ respectively.

Not only $\alpha(L)$ (12), but also an additional parameter γ_i was calculated using the formula

$$\gamma_i = \frac{1}{S_\lambda}\lambda_i, \qquad\qquad i = 1, ..., M \qquad (16)$$

where

$\quad S_\lambda$ – summed eigenvalues of the covariance matrix (13).

This parameter characterises the normalised spectrum of eigenvalues λ_i $(i = 1, ..., M)$ of the covariance matrix $c(z_i, z_j)$ and defines the contribution of the individual eigenvalues λ_i (modes, terms in expansion (7)) to the variability of the hydrophysical parameters under analysis.

Parameters $\alpha(L)$ (12) and γ_i (16) act as additional quantitative characteristics in the processing of the hydrological measurement data and will be used in further sections of this paper.

3. Approximation and visualisation of the vertical structure of temperature, salinity and density

This section discusses the structure of the eigenvalues of the covariance matrix, the plots of eigenfunctions h_k and amplitudes β_{ik}, and the convergence of expansions (7) and (15) in the approximation of the vertical structure of selected thermohaline parameters. The following example calculations were performed on the basis of *in situ* measurements done in the Faeroe-Shetland Channel in 1988.

3.1. Eigenvalues and the structure of eigenfunctions and amplitudes

Figs. 2 and 3 show plots of eigenfunctions (h_k) and amplitudes (β_{ik}) for seawater temperature, salinity and density calculated from *in situ* measurements in the Faeroe-Shetland Channel in 1988. The vertical structure
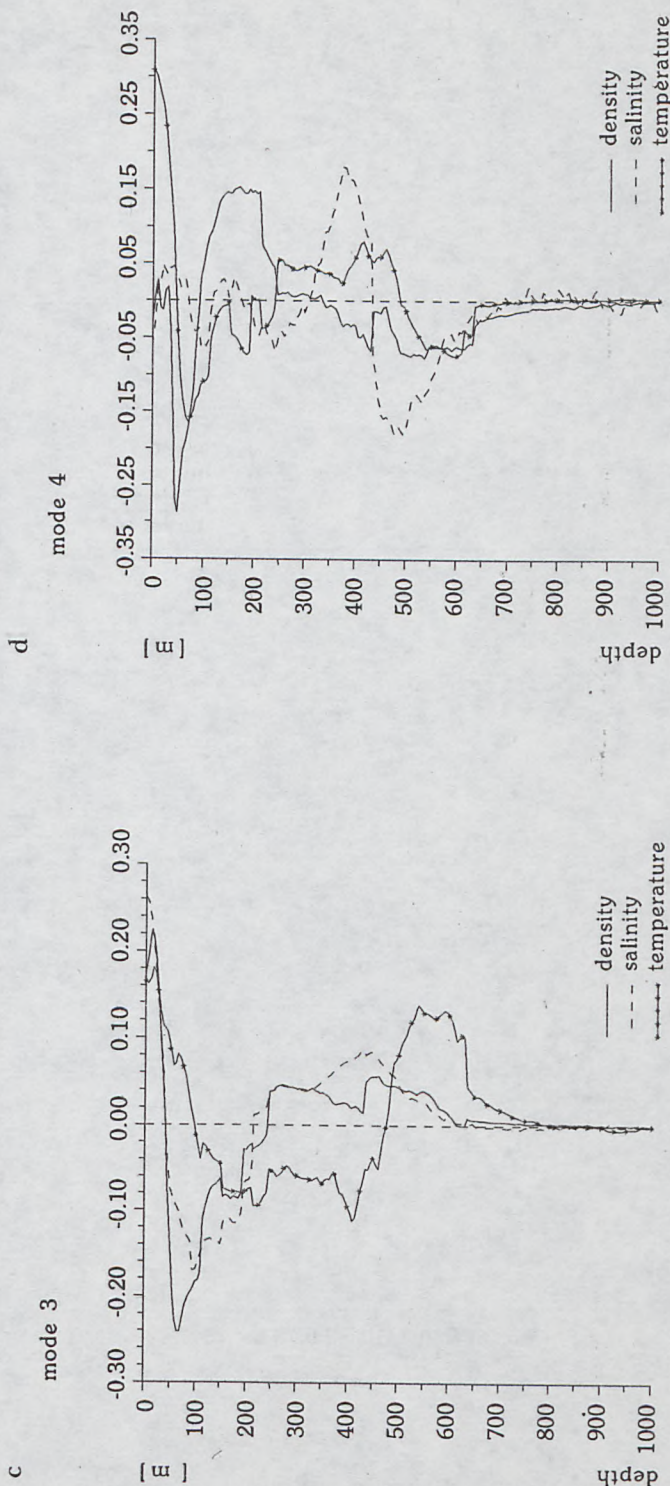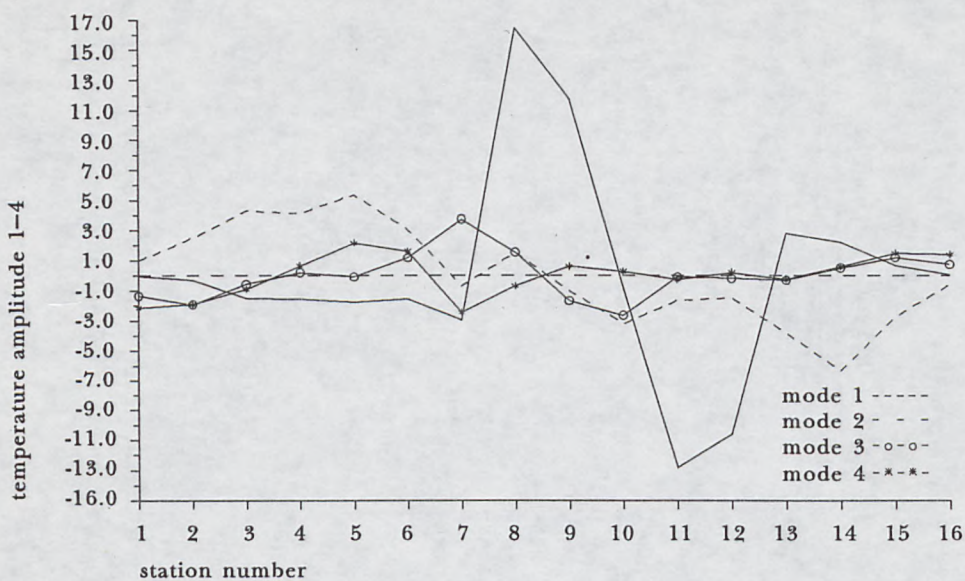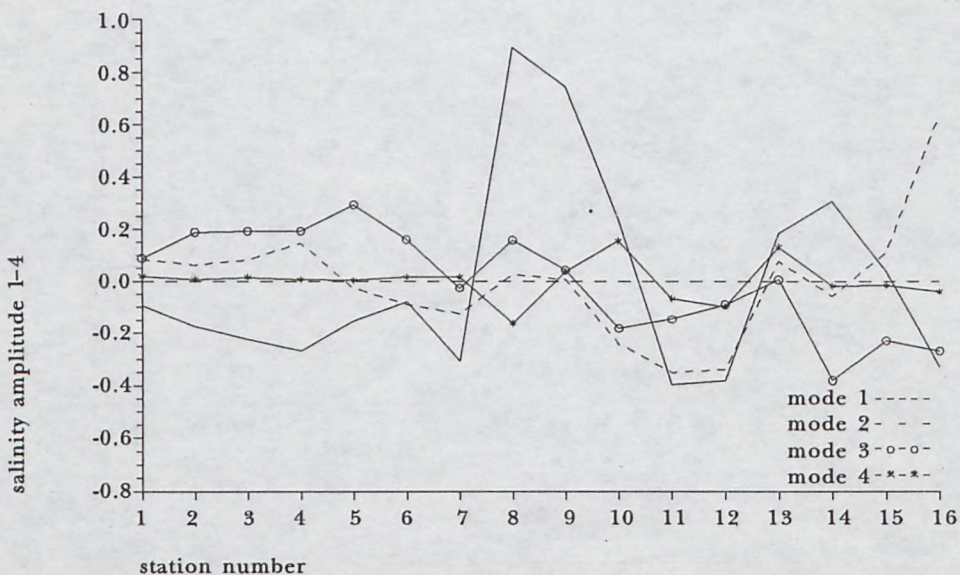
a
mode 1

b
mode 2
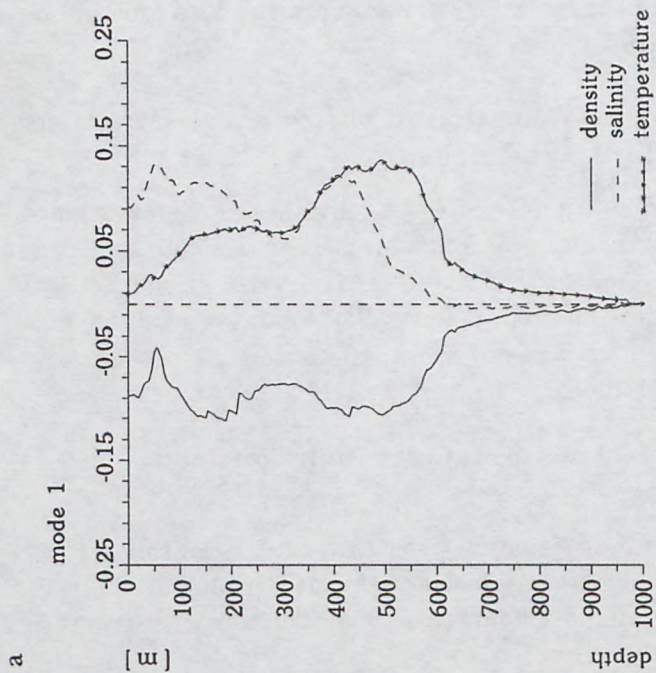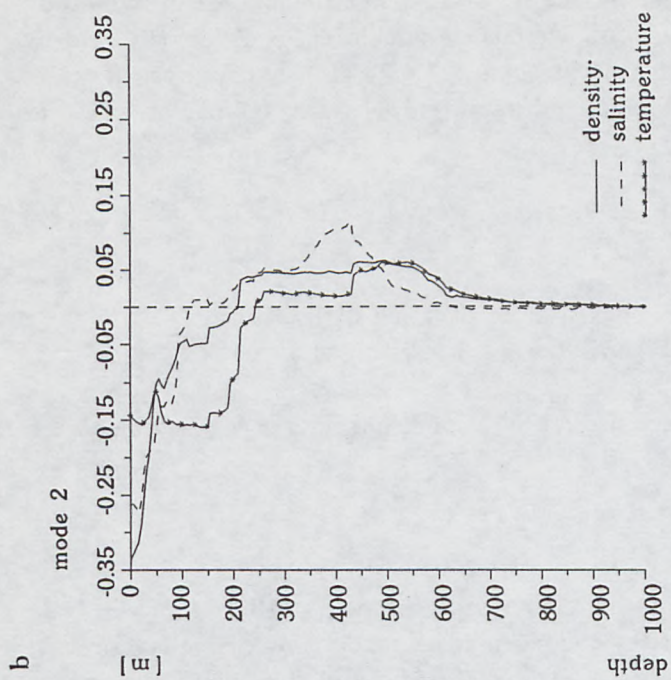
Fig. 2. Vertical structure of the first 4 water temperature, salinity and density eigenfunctions (modes) in a transect across the Faeroe-Shetland Channel (1988 measurement data): mode 1 (a), mode 2 (b), mode 3 (c), mode 4 (d)
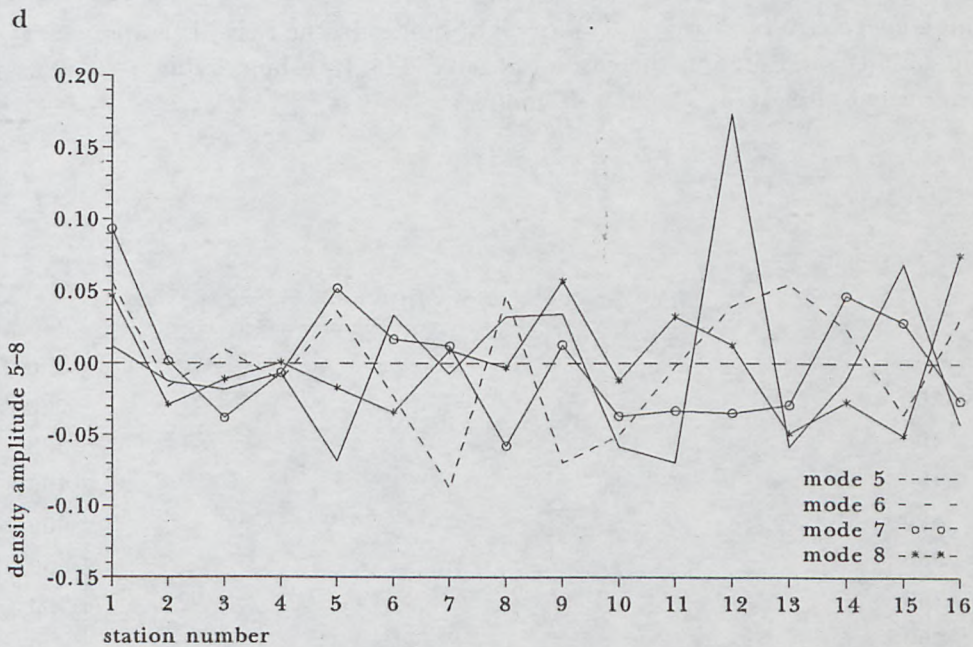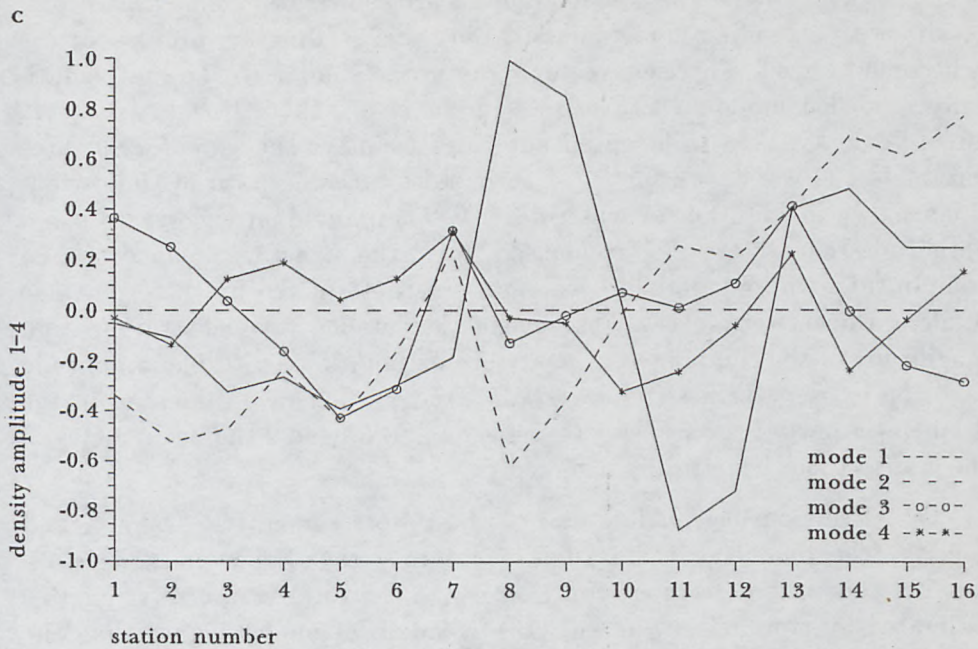
a

b

c

d

Fig. 3. Plots of the first 4 water temperature, salinity and density amplitudes and water density amplitudes 5–8 in a transect across the Faeroe-Shetland Channel (1988 measurement data): temperature amplitudes 1–4 (a), salinity amplitudes 1–4 (b), density amplitudes 1–4 (c), density amplitudes 5–8 (d)

of the eigenvectors for all three parameters are similar; they increase in complexity with ascending mode number, and the eigenfunction profiles for $i \geq$ 4 become blurred. The eigenvector structure is similar to the mathematically modelled mode structure (see Kundu *et al.*, 1975; Korotayev *et al.*, 1978; Pedlosky, 1978). The amplitude plots are much the same for all three parameters (Figs. 3a–c); for $i \geq 4$ their plots take the form of the oscillations shown in Fig. 3d for water density. The individual eigenvectors and amplitudes characterise in 'condensed' form the structure of uncorrelated components, whose variability scale power is determined by the eigenvalue λ_i along the entire transect. This reveals the detailed vertical structure and magnitude of the component at every profile point along it. The amplitude takes on extreme values (modes 1 and 2) at stations 8–11, located in the deep-water part of the transect (see Figs. 4 and 5, where the bathymetry of the transect is schematically depicted).

Tab. 1 sets out eigenvalues $\lambda_i, i = 1, .., 15$ for temperature, salinity and density (the final eigenvalue 16 is equal to zero). Eigenvalues decrease rapidly, and their percentage contribution to the total variance (strength), estimated by parameter γ_i in eq. (16), is small for modes higher than the 4th (Tab. 1). The values of the summed parameter $\alpha(L)$ (12) satisfy the convergence criterion ($\alpha \geq 99\,\%$) for eight modes in the case of temperature and salinity, and nine in the case of density. The threshold value $\alpha = 95\,\%$ is exceeded already by the first 4–5 modes.

a

salinity   [psu]
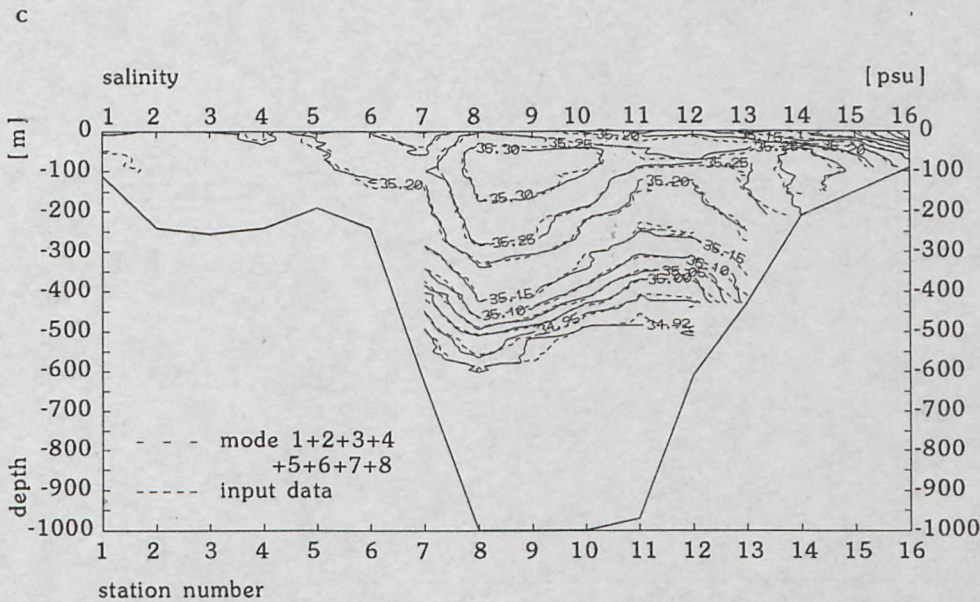
station number

b

c
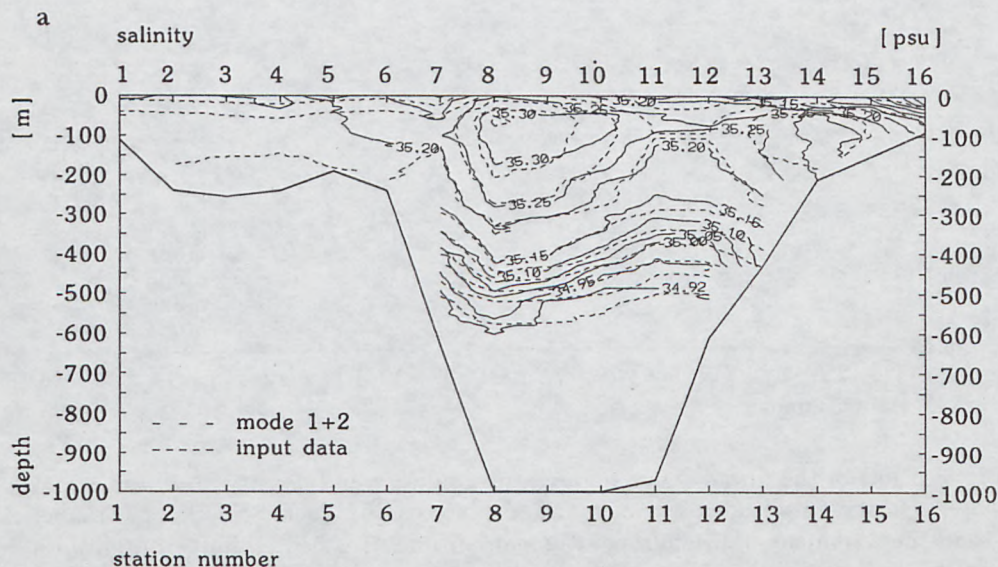
Fig. 4. Salinity distributions [psu] in a vertical transect across the Faeroe-Shetland Channel (1988 measurement data) for successively summed modes (from 1 to 8) illustrating expansion convergence by EOF (9). The solid isolines show the salinity distribution plotted on the basis of input data: sum of modes 1 and 2 (a), sum of modes 1–4 (b), sum of modes 1–8 (c)

a

b
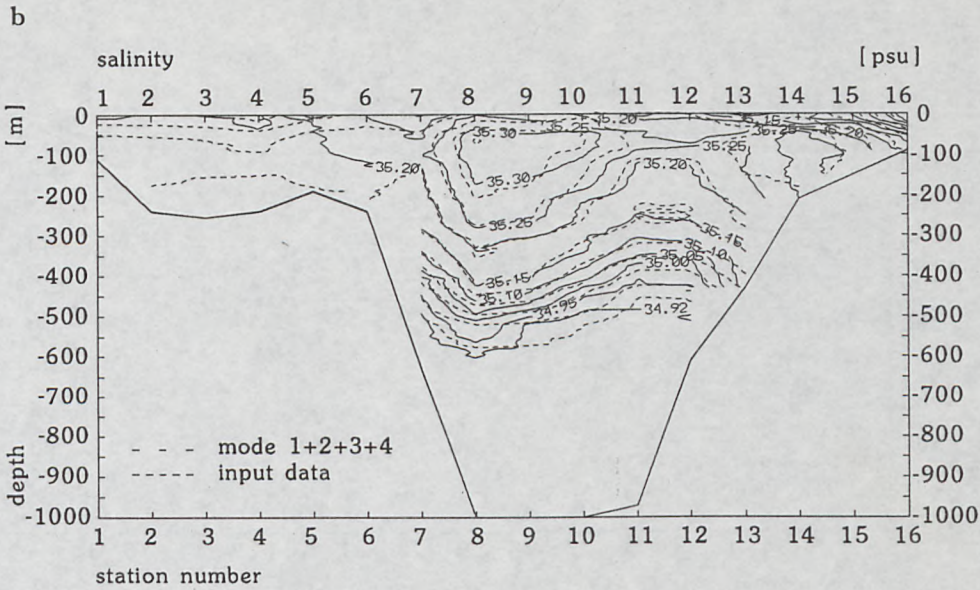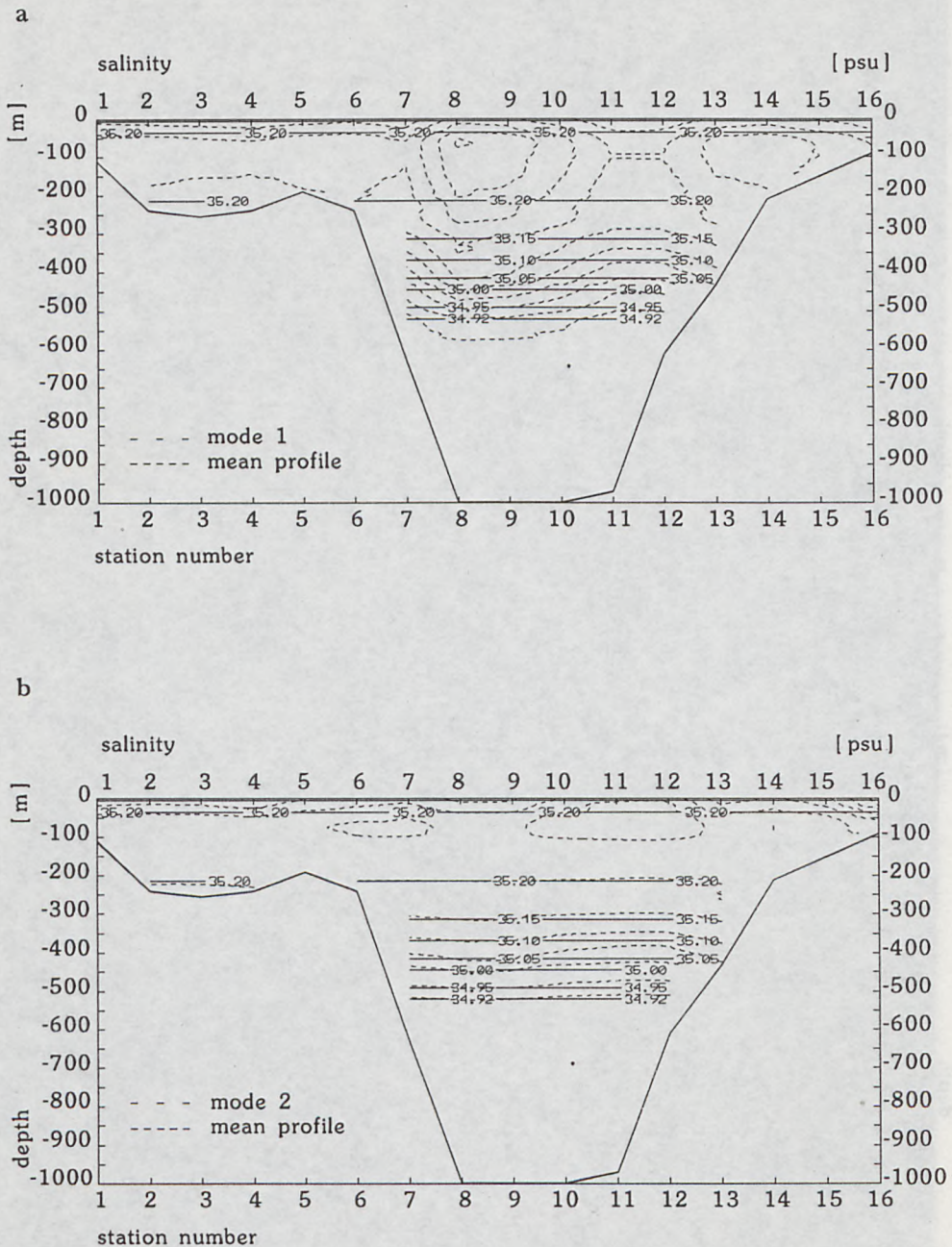

Fig. 5. Salinity distributions [psu] in a vertical transect across the Faeroe-Shetland Channel (1988 measurement data) for the discrete modes calculated from (15). The solid isolines show the salinity distribution plotted on the basis of the mean profile (1): mode 1 (a), mode 2 (b)

Table 1. Eigenvalues λ_i and their contribution $\gamma_i{}^*$ [%]; $\alpha_i{}^{**}$ [%] in the summed variance of temperature, salinity and density fluctuations in a transect across the Faeroe-Shetland Channel in 1988

No.	Temperature			Salinity			Density		
	λ_i	γ_i	α_i	λ_i	γ_i	α_i	λ_i	γ_i	α_i
1	716.9476	71.8	71.8	2.23612	57.7	57.7	3.34911	43.8	43.8
2	161.7152	16.2	80.0	0.79278	20.4	78.1	3.14954	34.9	78.7
3	35.2690	3.5	91.5	0.58933	15.2	93.3	0.92628	10.3	88.9
4	27.8667	2.8	94.3	0.08782	2.3	95.6	0.48708	5.4	94.3
5	20.8996	2.1	96.4	0.04907	1.3	96.9	0.15901	1.8	96.1
6	14.5447	1.5	97.9	0.04029	1.0	97.9	0.12145	1.3	97.4
7	7.9885	0.80	98.7	0.02561	0.66	98.6	0.06668	0.74	98.2
8	4.1003	0.41	99.1	0.01970	0.51	99.1	0.05706	0.63	98.8
9	3.6611	0.37	99.4	0.01023	0.26	99.4	0.03012	0.33	99.2
10	2.7385	0.27	99.7	0.00920	0.24	99.6	0.02498	0.28	99.4
11	1.0612	0.11	99.81	0.00811	0.21	99.8	0.02052	0.23	99.63
12	0.8276	0.08	99.89	0.00460	0.12	99.92	0.01483	0.16	99.79
13	0.4449	0.04	99.93	0.00167	0.04	99.96	0.00882	0.10	99.89
14	0.2745	0.03	99.97	0.00095	0.02	99.98	0.00512	0.06	99.95
15	0.1762	0.02	99.99	0.00041	0.01	99.99	0.00261	0.03	99.98

${}^*\gamma_i$ – estimated from eq. (16),
${}^{**}\alpha_i$ – estimated from eq. (12).

3.2. Vertical structure of temperature, salinity and density fields

The vertical salinity distributions along the transect (Fig. 4) calculated from (15) with an increasing number of modes (for $L = 1, ..., 8$) are illustrated by the convergence of expansion (7) on approximating the vertical profiles of water temperature, salinity and density σ_t by EOF. For comparison, Fig. 4 also shows isolines based on input data. Salinity was chosen to illustrate the calculations because it displays the greatest complexity of the vertical structure in this region (see Druet and Jankowski, 1991, 1992; Jankowski and Swerpel, 1990). Clearly, it is enough to take the first 4–5 terms (modes) of expansion (7) to describe the spatial structure of salinity (and temperature and density σ_t), although already the first mode provides the principal details of the structure. The remaining modes, which have an infinitesimal variance (see Tab. 1), contribute little and can be omitted from the practical calculations.

Fig. 5 provides a somewhat different picture, also based on salinity, of the contribution made by the various terms in expansion (7) to the spatial structure of hydrophysical fields. Depicting salinity plots for modes 1

and 2 (the first and second terms in expansion (7)) compared with the mean profile (1), Fig. 5 shows the structure details contributed by the various terms (modes) of expansion (7) and (16) describing ever smaller and weaker fluctuations to spatial distribution of the salinity along the vertical transect.

Approximated using expansion (7) and (15), water density profiles were used to estimate an important hydrological characteristic – transport of heat and mass across the transect. Tab. 2 sets out the volumes – calculated by the dynamic method (Zubov and Mamayev, 1956) – of water masses and quantities of heat for particular modes and for sums of consecutive modes (from 1 to 15) of density fluctuations. Analysis of the table confirms earlier observations, that in practical calculations the first 4–5 modes of density σ_t fluctuation field are sufficient to estimate geostrophic flows across a transect.

Table 2.* Volumes of water masses and heat transported through the vertical transect across the Faeroe-Shetland Channel in 1988 for the first 15 modes (reference level of no motion $z = 1000\,\text{m}$)

No.	Volume of water				Heat			
	A.O.		N.S.		A.O.		N.S.	
	$[10^6\ \text{m s}^{-1}]$	[%]	$[10^6\ \text{m s}^{-1}]$	[%]	$[10^{12}\ \text{J s}^{-1}]$	[%]	$[10^{12}\ \text{J s}^{-1}]$	[%]
1	−4.42	96.1	3.49	99.1	−121.9	97.7	115.6	97.2
2	−0.47	10.2	0.60	17.0	−14.9	11.9	21.4	18.0
3	−0.43	9.3	0.28	8.0	−11.5	9.2	8.2	6.8
4	−0.32	7.0	0.20	5.7	−8.8	7.1	5.8	4.9
5	−0.14	3.0	0.27	7.7	−4.1	3.3	8.0	6.6
6	−0.25	5.4	0.11	3.1	−5.5	4.4	2.9	2.4
7	−0.10	2.2	0.13	4.0	−2.9	2.4	4.1	3.4
8	−0.16	3.5	0.12	3.4	−3.5	2.8	2.6	2.2
9	−0.07	1.5	0.09	2.6	−1.9	1.5	2.6	2.2
10	−0.08	1.7	0.04	1.3	−1.6	1.3	1.0	0.86
11	−0.023	0.50	0.015	0.43	−0.55	0.44	0.35	0.29
12	−0.044	1.0	0.034	1.0	−0.97	0.78	0.83	0.70
13	−0.015	0.33	0.008	0.23	−0.45	0.36	0.23	0.19
14	−0.012	0.26	0.013	0.37	−0.27	0.22	0.27	0.23
15	−0.008	0.17	0.007	0.20	−0.20	0.16	0.18	0.15

* Note: positive values assumed for flows into the Norwegian Sea;
A.O. – into the Atlantic Ocean; N.S. – into the Norwegian Sea.

Fig. 6 shows $T - S$ graphs for the input data and for several separate modes. The figures also show the T – S plot for the mean profile. Such
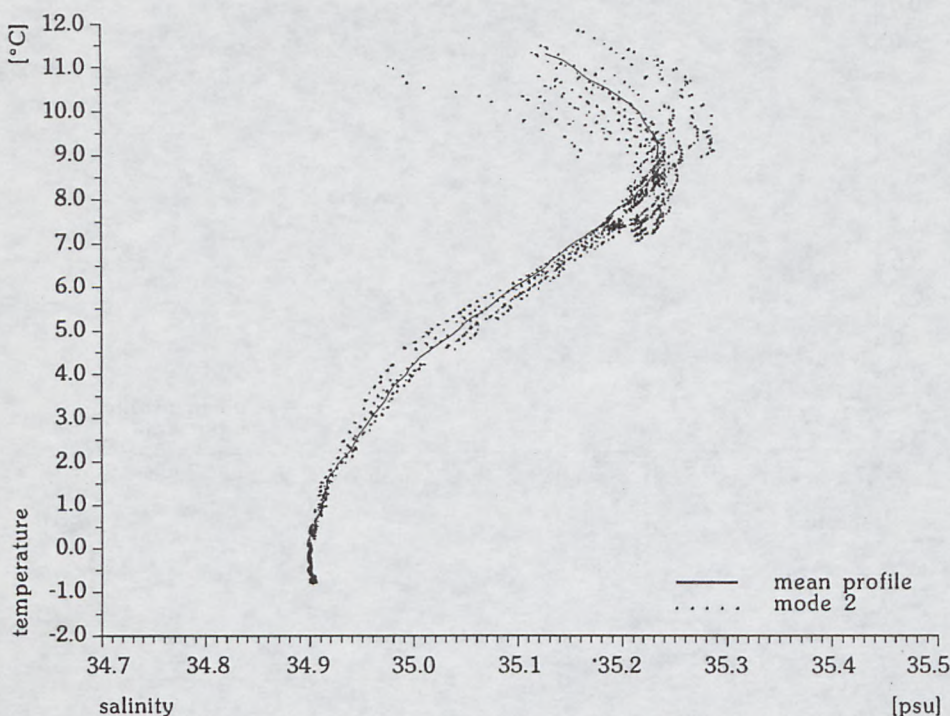
a

b
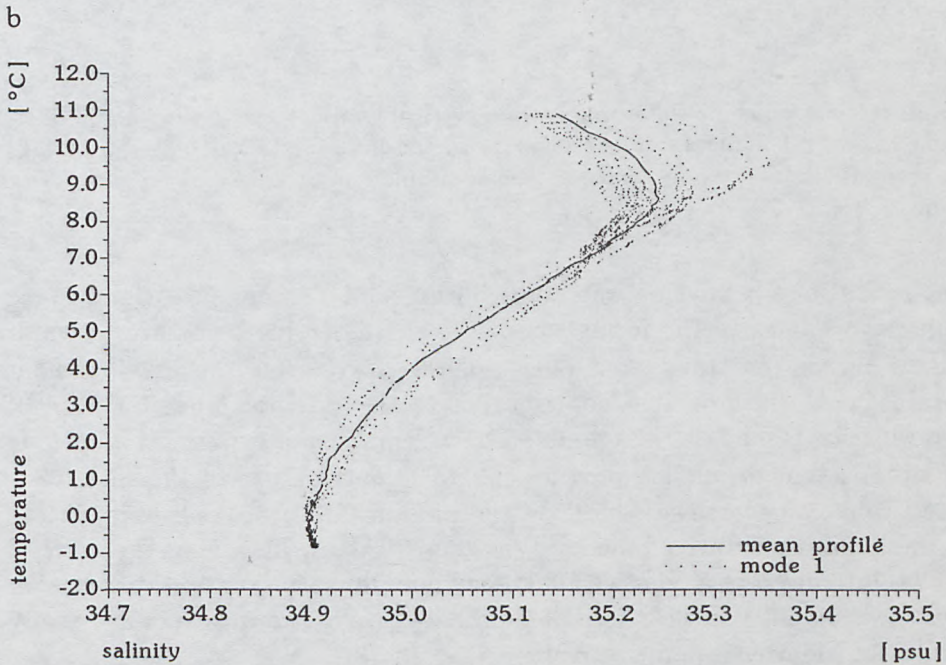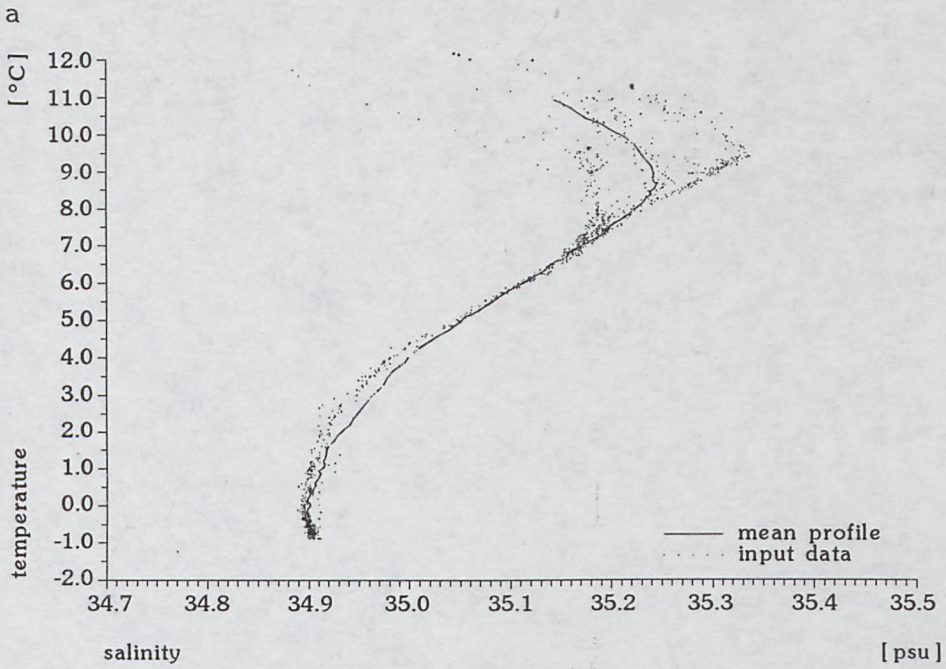
c

Fig. 6. $T - S$ graphs for water masses in a vertical transect across the Faeroe-Shetland Channel (1988 measurement data) for the discrete modes calculated from (15) for several discrete modes and the mean profile: input data (a), mode 1 (b), mode 2 (c)

graphs assist in analysing the contribution and defining the significance of discrete modes to the formation of the thermohaline structure of water masses on a given transect. Analysis of Fig. 6 confirms the previous conclusions, that the principal contribution to the thermohaline structure of water masses is made by the first 4–5 terms (modes) of expansion (7), while the others, though making only a negligible contribution to the total variance (Tab. 1), nevertheless indicate the presence of futher subtleties in the thermohaline structure of the study region's waters. Resolving the vertical profiles into discrete modes with a known maximum fluctuation variance allows the variability in the thermohaline structure of the waters of any study area to be identified quantitatively.

4. Variability of the thermohaline structure of waters in two transects across selected regions of the Norwegian Sea in 1988, 1989 and 1991

This section compares the variability of temperature, salinity and density σ_t in selected regions of the Norwegian Sea in the summers of 1988, 1989 and 1991. Because the eigenfunctions $h_k(z_j)$ and amplitudes β_{ik} of these parameters are structurally similar (see subsection 3.1), only the structural variability of the eigenvectors and amplitudes of density is used in the analysis of interannual variability.

4.1. The thermohaline structure of waters in the Faeroe-Shetland Channel in 1988, 1989 and 1991

Eigenvalues. Tab. 3 contains the 10 maximum eigenvalues λ_i for temperature, salinity and density taken from the 1988, 1989 and 1991 data, as
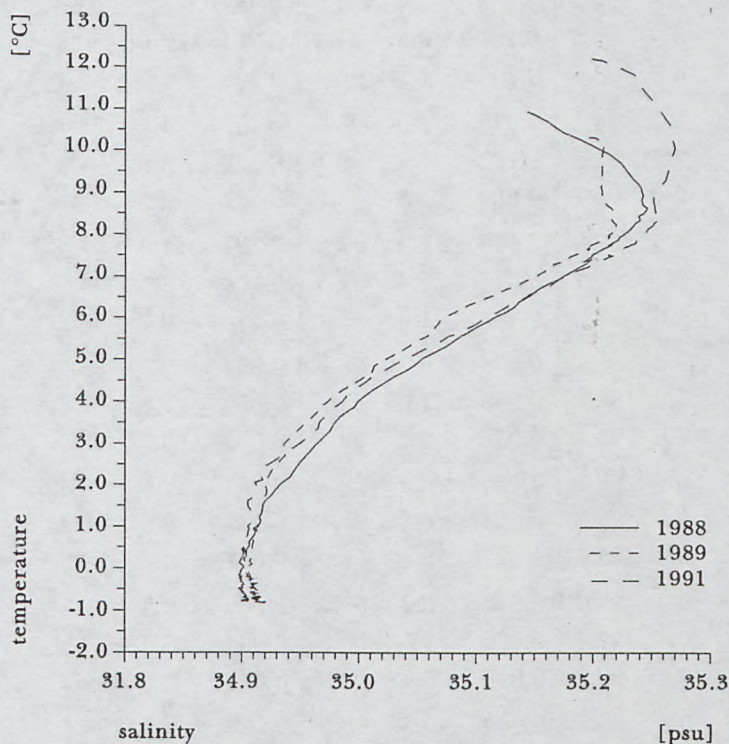

Fig. 7. $T - S$ graphs for water masses in a vertical transect across the Faeroe-Shetland Channel in 1988, 1989 and 1991 determined on the basis of mean profiles

Table 3. Eigenvalues λ_i and their contribution γ_i *[%]; α_i **[%] in the summed variance of temperature, salinity and density fluctuations in a transect across the Faeroe-Shetland Channel in 1988, 1989 and 1991

No.	Year	Temperature			Salinity			Density		
		λ_i	γ_i	α_i	λ_i	γ_i	α_i	λ_i	γ_i	α_i
1	1988	716.95	71.8	71.8	2.236	57.7	57.7	3.349	43.8	43.8
	1989	471.81	51.5	51.5	3.810	69.0	69.0	2.629	46.7	46.7
	1991	566.76	62.1	62.1	3.200	68.5	68.5	3.327	42.3	42.3
2	1988	161.72	16.2	80.0	0.792	20.4	78.1	3.150	34.9	78.7
	1989	259.38	28.3	79.8	0.806	14.6	83.6	1.661	29.5	76.2
	1991	171.78	18.8	80.9	0.999	21.4	89.9	2.829	36.0	78.3
3	1988	35.27	3.5	91.5	0.589	15.2	93.3	0.927	10.3	88.9
	1989	79.50	8.7	88.5	0.396	7.2	90.8	0.536	9.5	85.7
	1991	75.86	8.3	89.2	0.140	3.0	92.9	0.717	9.1	87.4
4	1988	27.87	2.8	94.3	0.088	2.3	95.6	0.487	5.4	94.3
	1989	48.56	5.3	93.8	0.191	3.5	94.3	0.254	4.5	90.3
	1991	40.71	4.5	93.6	0.108	2.3	95.2	0.368	4.7	92.1
5	1988	20.90	2.1	96.4	0.049	1.3	96.9	0.159	1.8	96.1
	1989	19.81	2.2	95.9	0.102	1.8	96.1	0.220	3.9	94.2
	1991	18.63	2.0	95.7	0.069	1.5	96.7	0.231	2.9	95.0
6	1988	14.54	1.5	97.9	0.040	1.0	97.9	0.121	1.3	97.4
	1989	11.73	1.3	97.2	0.076	1.4	97.5	0.145	2.6	96.7
	1991	16.61	1.6	97.3	0.048	1.0	97.7	0.174	2.2	97.2
7	1988	7.99	0.8	98.7	0.026	0.7	98.6	0.067	0.7	98.2
	1989	9.06	1.0	98.2	0.056	1.0	98.5	0.059	1.0	97.8
	1991	7.64	0.8	98.1	0.032	0.7	98.4	0.059	0.7	98.0
8	1988	4.10	0.4	99.1	0.020	0.5	99.1	0.057	0.6	98.8
	1989	5.71	0.6	98.8	0.031	0.6	99.1	0.035	0.6	98.4
	1991	5.52	0.6	98.7	0.022	0.4	98.9	0.052	0.7	98.6
9	1988	3.66	0.4	99.4	0.010	0.3	99.4	0.030	0.3	99.1
	1989	5.22	0.6	99.4	0.026	0.5	99.5	0.034	0.6	99.0
	1991	4.27	0.5	99.2	0.020	0.4	99.3	0.042	0.5	99.2
10	1988	2.74	0.3	99.7	0.009	0.2	99.6	0.025	0.3	99.4
	1989	2.14	0.2	99.6	0.012	0.2	99.8	0.019	0.3	99.3
	1991	2.98	0.3	99.5	0.012	0.3	99.6	0.025	0.3	99.5

*γ_i – estimated from eq. (16),
**α_i – estimated from eq. (12).
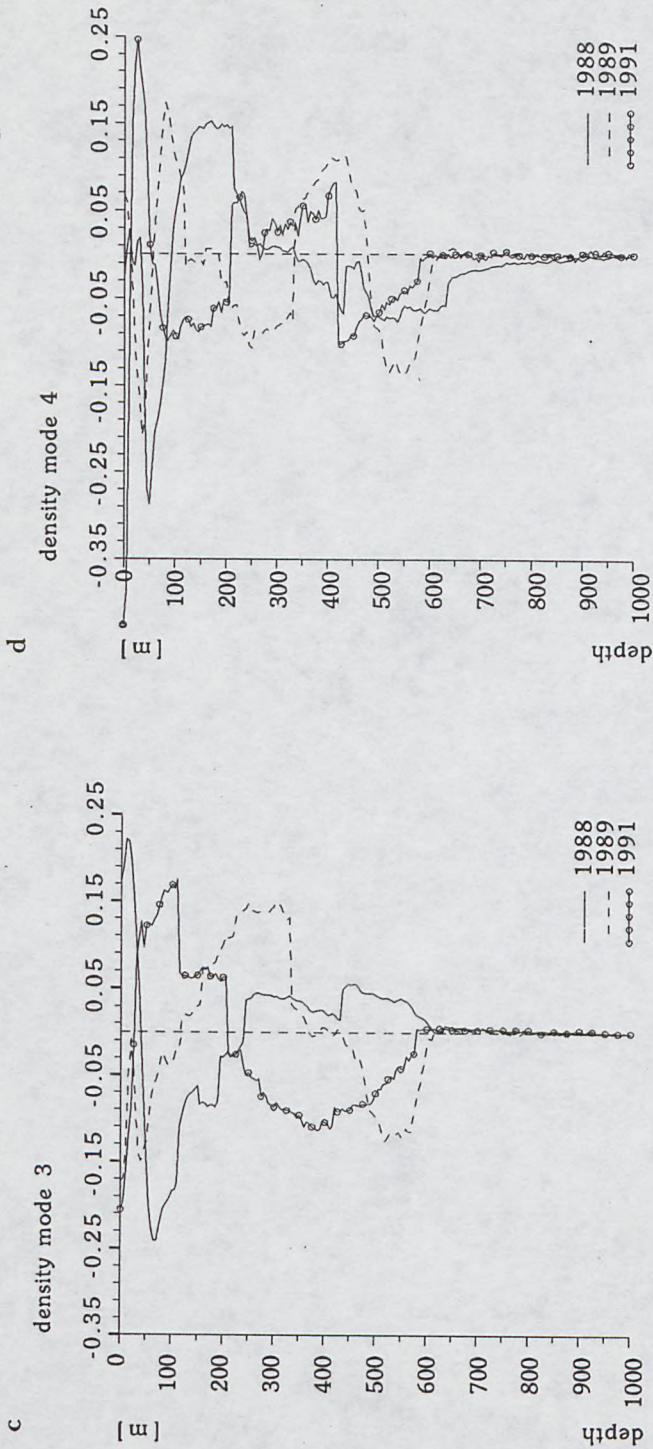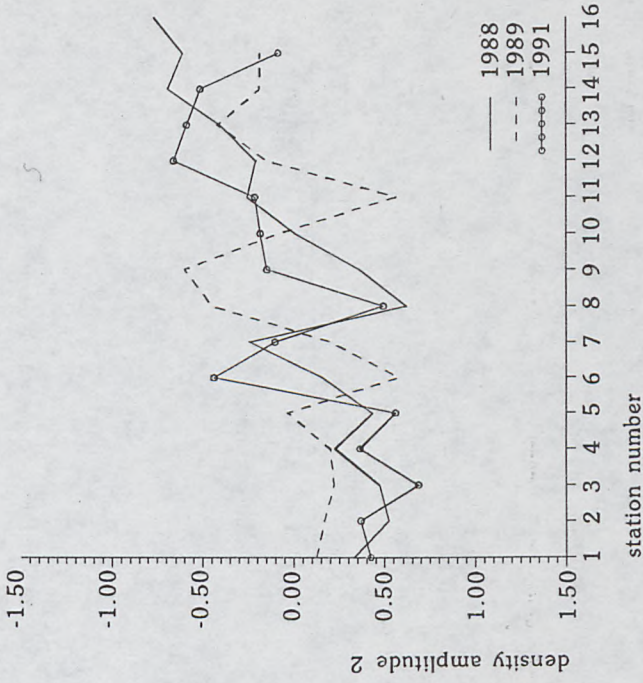
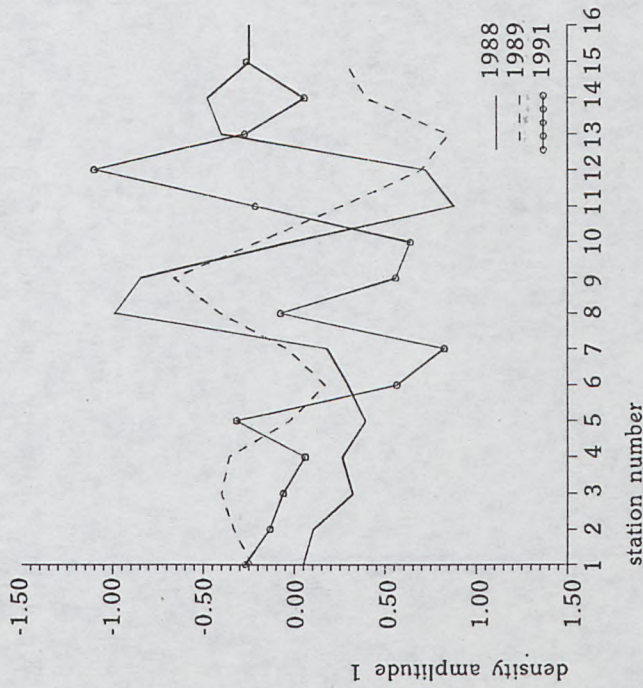a — density mode 1
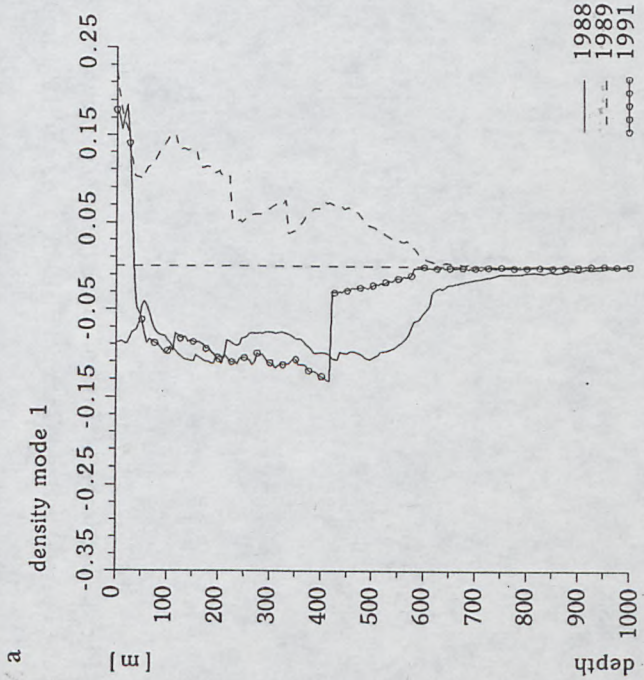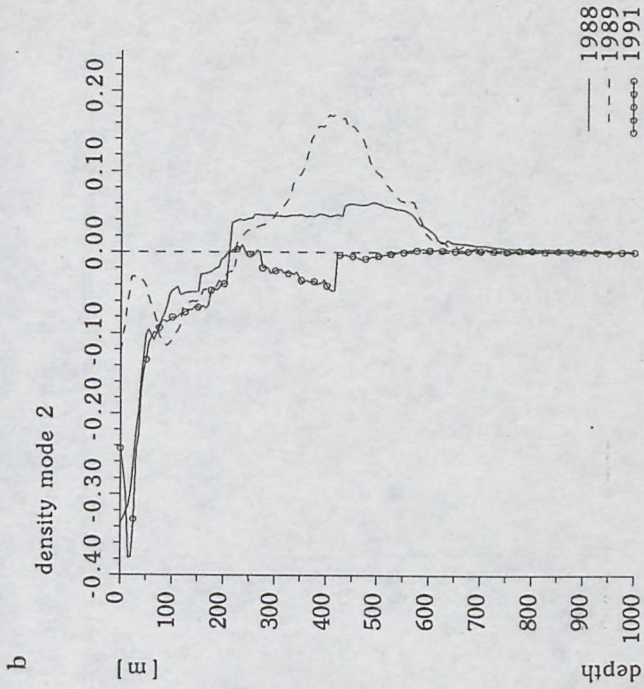
b — density mode 2

Fig. 8. Vertical structure of the first 4 eigenfunctions (vertical modes) for water density in a transect across the Faeroe-Shetland Channel in 1988, 1989 and 1991: mode 1 (a), mode 2 (b), mode 3 (c), mode 4 (d)

a — density amplitude 1, station number, 1988 1989 1991

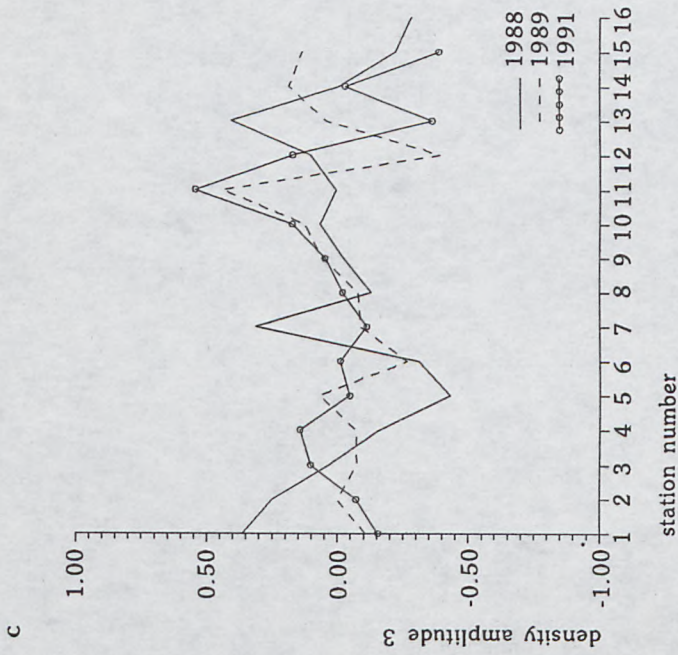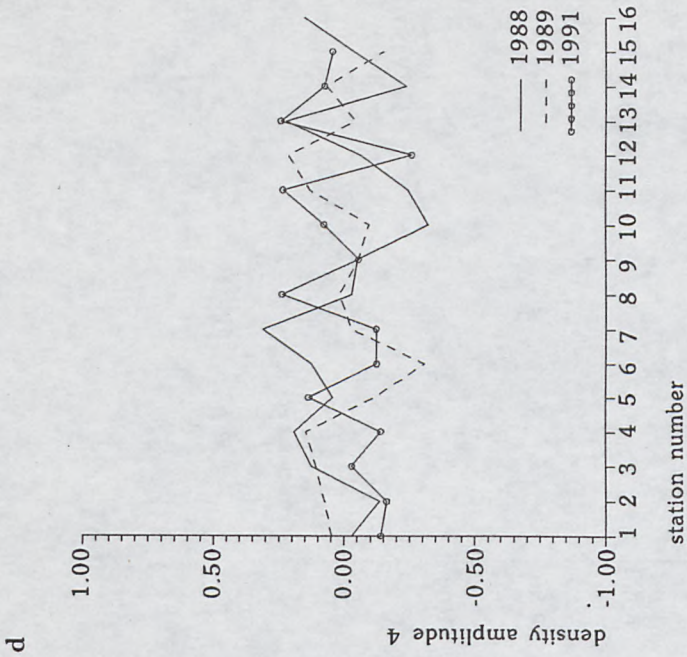b — density amplitude 2, station number, 1988 1989 1991

Fig. 9. Plots of the first 4 water-density amplitudes in a transect across the Faeroe-Shetland Channel in 1988, 1989 and 1991: amplitude 1 (a), amplitude 2 (b), amplitude 3 (c), amplitude 4 (d)

well as the values of parameters γ_i i α_i. The orders of magnitude of the eigenvalues and their structure are similar for all 3 years and the quantities measured. The parameters γ_i and α_i indicate differences in the distribution of the term in the processes characterising variability. The greatest differences in eigenvalues are in modes 1–4, which leads to differences in the convergence rate of the series approximating the vertical profile (7) (Tab. 3). However, the results of calculations based on the 1989 data are distinctive.

$T - S$ **graphs.** Fig. 7 shows the $T - S$ graph plotted for the mean profiles determined from the 1988, 1989 and 1991 data. This graph characterises the thermohaline structure of the water masses (hydrological background) along the transect in the various years.

Eigenfunctions and amplitudes. Fig. 8 shows the plots of the first 4 eigenvectors h_k for density σ_t fluctuations in each year. The curves are much the same in shape with respect to both years and parameter. The vertical structure of the 1989 eigenvectors is distinctive, especially in the first mode. Fig. 9 shows the plots of the first 4 amplitudes β_{ik} of density σ_t fluctuation modes in each year. There are noticeable differences in the values and plot shape from the various stations on the transect. The maximum amplitudes (mode 1) in 1988 and 1989 data occur in the region of the deep-water stations 8–11. In 1991 extreme amplitudes were recorded at stations 10–14 (in shallower regions).

4.2. The thermohaline structure of waters in the confluence zone of the Norwegian and Barents Sea in 1988, 1989 and 1991

Eigenvalues. Tab. 4 sets out the 10 maximum eigenvalues λ_i and parameters γ_i and α_i of temperature, salinity and density from the 1988, 1989 and 1991 data. The order of magnitude of the eigenvalues and their structure are similar for the years and parameters in question, although γ_i and α_i indicate differences in the internal structure of the processes characterising variability. There are large differences in the magnitude of the eigenvalues of all the parameters in the 1991 data, and are most distinctive in the case of temperature and salinity fluctuactions, especially in modes 1–4. Furthermore, the values and structure of γ_i and α_i are indicative of differences in the internal structure of the processes characterising variability in the quantities analysed. The contribution of the first three eigenvalues to the summed variance differs from that of the other two years; the first value, especially, is considerably smaller. In the case of density fluctuactions the first three values also deviate from the structure of the other years. The upshot of this are the differences in the convergence rate of series (7) (see Tab. 4).

Table 4. Eigenvalues λ_i and their contribution γ_i *[%]; α_i **[%] in the summed variance of temperature, salinity and density fluctuations along longitude 15° E (from 70° N to 76° 30′ N) in 1988, 1989 and 1991

No.	Year	Temperature			Salinity			Density		
		λ_i	γ_i	α_i	λ_i	γ_i	α_i	λ_i	γ_i	α_i
1	1988	1389.03	73.1	73.1	4.567	58.7	58.7	19.996	77.2	77.2
	1989	1601.03	62.7	62.7	11.510	67.7	67.7	21.878	83.3	83.3
	1991	368.42	49.6	49.6	1.021	43.2	43.2	4.467	65.1	65.1
2	1988	232.20	12.2	85.4	1.043	23.7	82.4	3.332	12.9	90.1
	1989	517.15	20.2	82.9	2.213	13.0	80.7	1.860	7.1	90.4
	1991	218.15	29.4	79.0	0.620	26.3	69.5	1.334	18.6	83.7
3	1988	99.09	5.2	90.6	0.530	6.8	89.2	0.845	3.3	93.3
	1989	242.43	9.5	92.4	1.427	8.4	89.1	0.916	3.5	93.8
	1991	67.23	9.0	88.0	0.582	16.0	85.5	0.582	8.1	91.8
4	1988	74.95	3.9	94.5	0.321	4.1	93.3	0.698	2.7	96.0
	1989	95.30	3.7	96.2	1.033	6.1	95.2	0.587	4.5	96.1
	1991	39.05	5.3	93.3	0.136	5.8	91.3	0.251	3.5	95.3
5	1988	38.52	2.0	96.6	0.178	2.3	95.6	0.413	1.6	97.6
	1989	35.24	1.4	97.5	0.391	2.3	97.5	0.337	1.3	97.4
	1991	23.08	3.1	96.4	0.115	3.7	95.0	0.115	1.6	96.9
6	1988	32.18	1.7	98.3	0.111	1.4	97.0	0.211	0.8	98.4
	1989	32.65	1.3	98.8	0.187	1.1	98.6	0.289	1.1	98.5
	1991	12.53	1.7	98.1	0.046	2.0	97.0	0.073	1.0	97.9
7	1988	16.44	0.9	99.1	0.079	1.0	98.0	0.177	0.6	99.1
	1989	13.24	0.5	99.3	0.143	0.8	99.4	0.155	0.6	99.1
	1991	6.04	0.8	98.9	0.023	1.0	98.0	0.053	0.7	98.6
8	1988	6.64	0.4	99.5	0.063	0.8	98.8	0.096	0.4	97.5
	1989	7.68	0.3	99.6	0.039	0.2	99.6	0.092	0.4	99.1
	1991	2.58	0.4	99.2	0.017	0.7	98.7	0.032	0.4	99.1
9	1988	5.40	0.2	99.8	0.033	0.4	99.2	0.054	0.2	99.7
	1989	4.13	0.2	99.8	0.020	0.1	99.7	0.067	0.2	99.7
	1991	2.05	0.3	99.5	0.009	0.4	99.1	0.025	0.4	99.4
10	1988	1.96	0.1	99.9	0.030	0.4	99.6	0.035	0.1	99.8
	1989	2.94	0.1	99.9	0.017	0.1	99.8	0.040	0.2	99.8
	1991	1.41	0.2	99.7	0.008	0.3	99.4	0.014	0.2	99.6

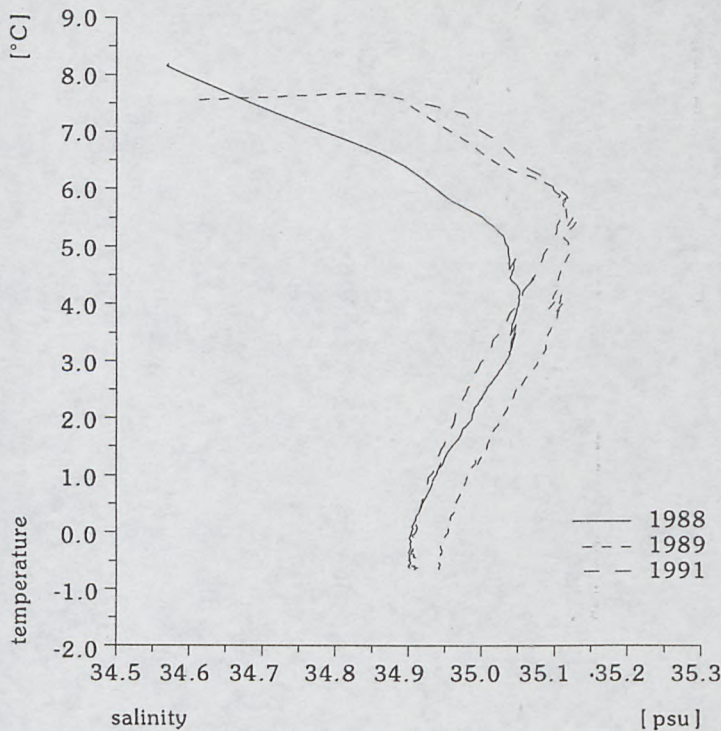*γ_i – estimated from eq. (16),
**α_i – estimated from eq. (12).

Fig. 10. $T - S$ graphs for water masses in a vertical transect along longitude $15°$E (from $70°$ N to $76°$ $30'$ N) in 1988, 1989 and 1991 determined on the basis of mean profiles

$T - S$ **graphs.** Fig. 10 presents the $T - S$ graph for the mean profiles determined from the 1988, 1989 and 1991 data. It characterises the thermohaline structure of water masses (hydrological background) along the transect in each year. The greatest differences were recorded in sub-surface layer (temperature $T \geq 5°$C and salinity $S \geq 35.05$ psu) in 1989. In the surface layer however, mean conditions were very much the same in 1989 and 1991.

Eigenfunctions and amplitudes. Fig. 11 shows the plots of the first 4 eigenvectors h_k of density σ_t fluctuations in each year. The vertical distributions of the curves are similar for the various years and parameters. However, the vertical structure of the 1989 eigenvectors, particularly in the first two modes, is distinctive. Fig. 12 presents the plots of the first 4 amplitudes β_{ik} of density σ_t in the different years. The curves plotted from

a

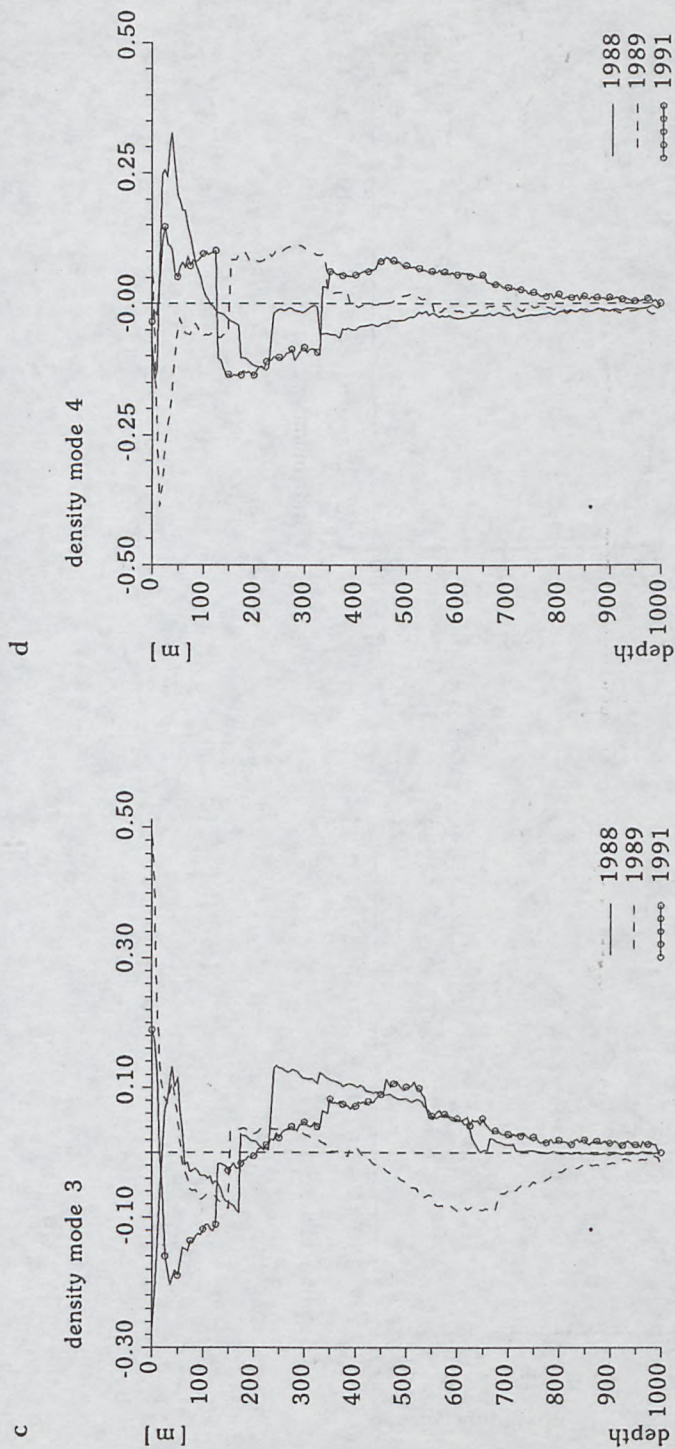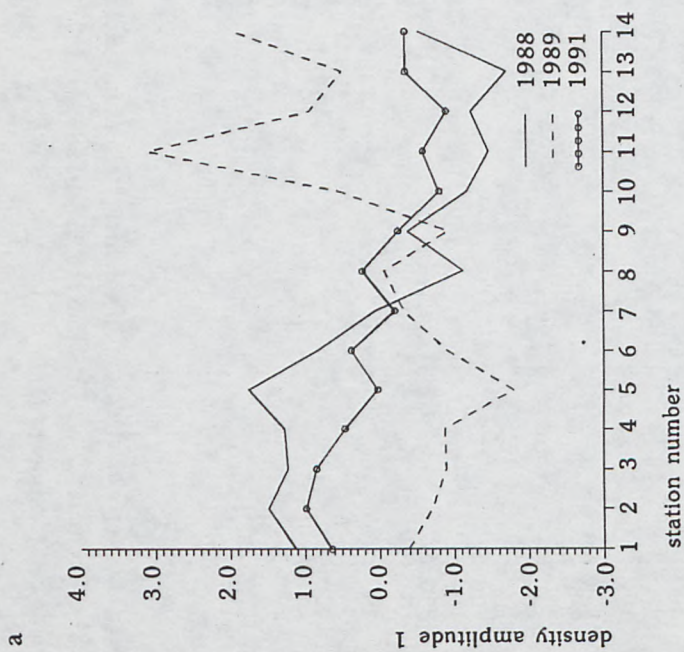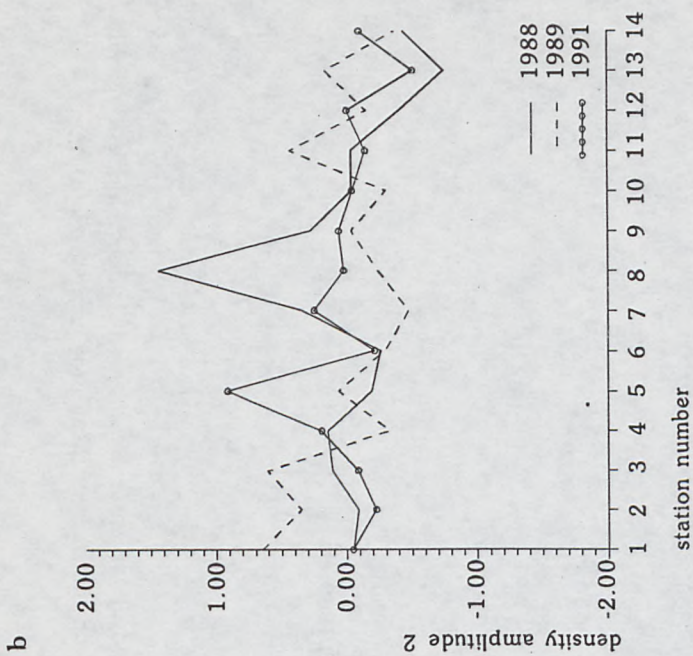density mode 1

b
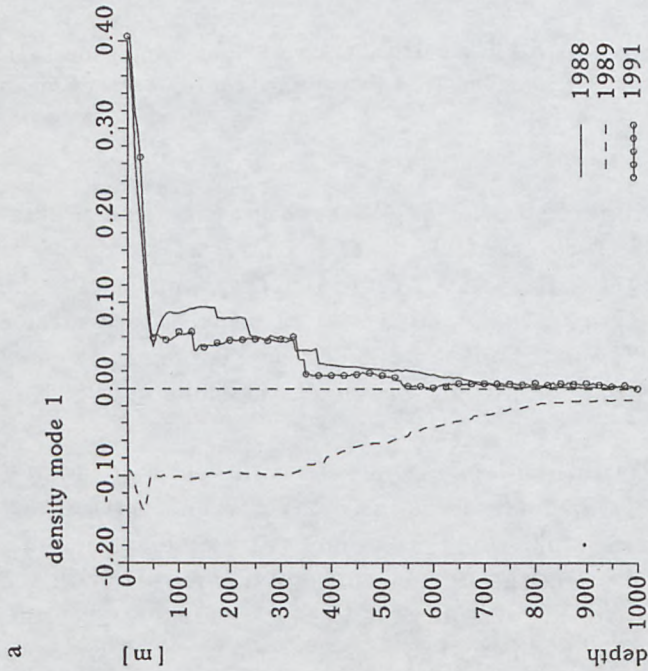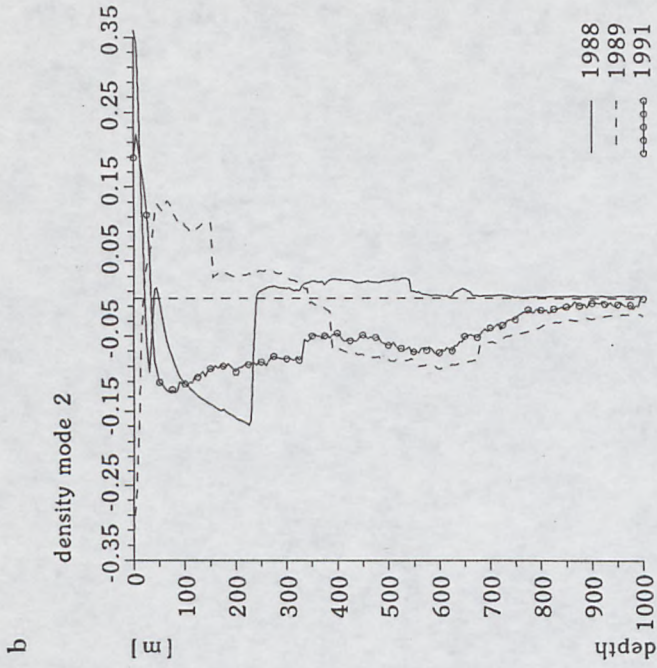
density mode 2

Fig. 11. Vertical structure of the first 4 eigenfunctions (vertical modes) for water density in a transect along longitude 15° E (from 70° N to 76° 30′ N) in 1988, 1989 and 1991 determined on the basis of mean profiles: mode 1 (a), mode 2 (b), mode 3 (c), mode 4 (d)
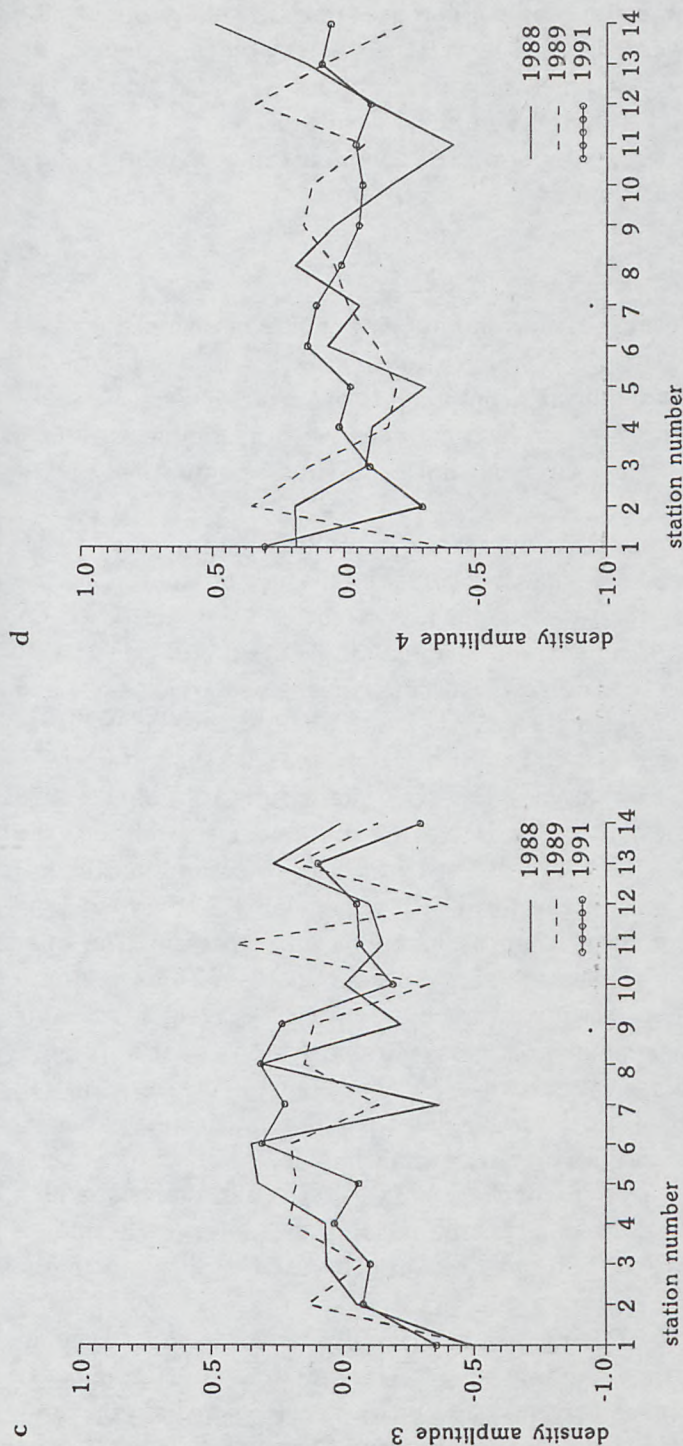
Fig. 12. Plots of the first 4 water-density amplitudes in a vertical transect along longitude 15° E (from 70° N to 76° 30′ N) in 1988, 1989 and 1991 determined on the basis of mean profiles: amplitude 1 (a), amplitude 2 (b), amplitude 3 (c), amplitude 4 (d)

the 1989 data, especially those in the first two modes, are clearly different. In the remaining modes there are some differences both in values and in plot shape; such differences were recorded at various stations on the transect. In 1989, amplitude (mode 1) attained maximum values in the region of the stations 3–7 and 10–13. The amplitude curves plotted from the 1988 and 1991 data are similar (especially modes 1 and 2) and attain maximum values in the region of stations 3–6, minima in the region of stations 12–14.

5. Conclusions

EOF are used to determine uncorrelated components of decreasing variance characterising the 'energy' (strength) of fluctuation in a given quantity. In this way the most significant components of variability can be separated and the insignificant, often parasitical ones, with negligible variance, can be filtered out. *In situ* measurement data can thus be smoothed out to a given accuracy.

By separating uncorrelated components of different amplitude (variance), one can visualise the small structural details in the spatial distributions of hydrophysical quantities along a transect, in a profile or $T - S$ graph, and compare spatial and temporal variabilities of different data sets. EOF data analysis of selected transects has confirmed the inferences reached by means of standard hydrological analysis (Druet and Jankowski, 1992) regarding the different thermohaline conditions obtaining in 1988, especially in the confluence zone. The closeness of EOF characteristics for the 1988 and 1991 data also show that in the latter measurement period too, the thermohaline structure of the water differed from that recorded in 1989.

Presenting the data sets in the form of a expansion (7) makes it possible to economise on memory when archiving them, especially the ones containing a large number of parameters (measurement stations and levels). Large sets can be described by means of a limited set of eigenfunctions and amplitudes. Because dependences are separated from variables z and x, approximation of hydrophysical quantities by expansion (7) makes it easy to perform mathematical operations on the data, *e.g.* differentiating, essential in the analysis of water stability or in estimating field smoothness. Amplitude functions can be used in correlation and statistical analysis, which raises the value of comparative analysis in variability studies of thermohaline parameters. Both sets of functions can also be used to fill gaps in the measurement data.

These applications of EOF require statistically realiable measurement data to be available so that a stable set of eigenfunctions and amplitudes can be determined. The investigations of other workers (see *e.g.* Glukhovskiy and Fortus, 1982) indicate that sets containing measurements from at least

80–100 profiles have to be analysed. The results of calculations can then be used to model the field structure of hydrophysical quantities. The empirical material obtained from cruises of r/v 'Oceania' was insufficient for these purposes.

Summarising, EOF do contribute some new aspects to the study of the structural variability of temperature, salinity and density field in sea water, and enable the variability components making up the fluctuation field to be assessed with greater reliability.

References

Druet C., Jankowski A., 1992, *Some results of three-year investigations on the interannual variability of the Norwegian – Barents confluence zone*, Pol. Polar Res., 13 (1), 3–17.

Pedlosky J., 1987, *Geophysical fluid dynamics*, Second edition, Springer Verlag, New York.

Druet C. (ed.), 1993, *Results of Polish three-year oceanographic investigations of the interannual variability of Greenland Sea energoactive zones*, Stud. i Mater. Oceanol., 65, 1–223.

Druet C., Jankowski A., 1991, *Flow across south and east boundaries of the Norwegian Sea*, Oceanologia, 30, 37–46.

Glukhovskiy A. B., Fortus M. I., 1982, *Otsenka statisticheskoy nadyozhnosti empiricheskikh ortogonalnykh funktsiy*, Izv. AN SSSR, ser. Fiz. Atm. i Okeana, 18 (5), 451–459.

Holmstrom I., 1963, *On a method for parametric representation of state of the atmosphere*, Tellus, 15 (2), 127–149.

Jankowski A., 1991a, *Thermohaline structure and water circulation in the contact area between the Norwegian Sea and the Barents Sea in summer 1988*, Stud. i Mater. Oceanol., 58, 169–185.

Jankowski A., 1991b, *Thermohaline structure and water circulation in the Faeroe-Shetland Channel in summer 1988*, Stud. i Mater. Oceanol., 58, 153–167.

Jankowski A., Swerpel S., 1990, *Selected problems of the thermohaline structure and dynamics of the water masses in Norwegian and Greenland Seas*, Pol. Polar Res., 11 (1–2), 3–16.

Johannessen O. M., 1986, *Brief overview of the physical oceanography*, [in:] *The Nordic Seas*, B. G. Hurdle (ed.), Springer Verlag, New York–Berlin, 103–127.

Korotayev G. K., Kosnyrev V. K., Yusupova T. A., 1978, *Ob ustoychivosti vertikalnoy struktury vozmushcheniy polya temperatury sinopticheskikh vikhrey*, [in:] *Eksperimentalnye issledovaniya po mezhdunarodnoy programme 'Polimode'*, Mor. Gidrofiz. Inst., Sevastopol, 55–63.

Kundu P. K., Allen J. S., Smith R. L., 1975, *Modal decomposition of the velocity field near the Oregon Coast*, J. Phys. Oceanogr., 5 (4), 683–704.

Lorenz E. N., 1956, *Empirical orthogonal function and statistical weather*, Sci. Rept. No. 1, Statistical Forecasting Project, Mass. Inst. Tech., Dept. of Meteorology, Cambridge.

Nielsen P. B., 1979, *On empirical orthogonal functions (EOF) and their use for analysis of the Baltic sea level*, Københavns Universitet, Institut for Fysisk Oceanografi, Report No. 40.

Obukhov A. N., 1960, *O statisticheskich ortogonalnykh rozlozheniyakh empiricheskikh funktsiy*, Izv. AN SSSR, ser. Geofizicheskaya, 3, 432–439.

Preisendorfer R. W., 1988, *Principal component analysis in meteorology and oceanography*, Elsevier, Amsterdam–Oxford–New York–Tokyo.

Ralston A., 1975, *Introduction to numerical analysis*, PWN, Warszawa, (in Polish).

Sukhovey V. F., 1977, *Izmenchivost gidrologicheskikh usloviy Atlanticheskogo okeana*, Izd. Nauk. Dumka, Kiyev.

UNESCO, 1983, *Algorithms for the computation of fundamental properties of sea water*, UNESCO Tech. pap. mar. sci., 44.

Vasilenko V. M. Mirabel A. P., 1976, *O parametrizatsii vertikalnoy struktury techeniy v Tropicheskoy Atlantike s pomoshchyu statisticheskikh ortogonalnykh funktsiy*, Okeanologiya, 6 (2), 222–228.

Wróblewski A., 1984, *Application of empirical orthogonal functions to decomposition of sea level changes in the Gulf of Gdańsk*, Stud. i Mater. Oceanol., 43, 135–148, (in Polish).

Wróblewski A., 1986, *Application of EOF to computations of the storm surges on the Polish Baltic coast in January 1983*, Acta Geophys. Pol., XXXIV (1), 63–76.

Wróblewski A., 1990, *Statistical forecasting of random dynamic processes in the near-shore zone of the South Baltic*, Ossolineum, Wrocław–Warszawa–Kraków, (in Polish).

Zubov N. N., Mamayev O. I., 1956, *Dinamicheskiy metod vychisleniya elementov morskikh techeniy*, Gidrometeoizdat, Leningrad.